P = pressure
r = radius
r_G = radius at which gas-liquid interface is located
r_W = pipe radius
u = velocity in liquid film measured with respect to gas bubble
u_D = dimensionless velocity, $u/(v_G + v_L + w)$
v = velocity in liquid film measured with respect to pipe wall
v_B = bubble-rise velocity
v_G = superficial gas velocity
v_L = superficial liquid velocity
V = dimensionless velocity, $w/(v_G + v_L + w)$
w = velocity of gas bubble through surrounding liquid
z = vertical distance from bubble head
z_D = dimensionless vertical distance, $zg/(v_G + v_L + w)^2$

Greek Letters

β = dimensionless area occupied by gas bubble, r_G^2/r_W^2
η = dimensionless radius, r/r_W
λ = cumulative volumetric liquid holdup
μ = liquid viscosity
ρ = liquid density
ϕ = functional dependence
Φ = functional dependence
Ψ = functional dependence
σ = surface tension

Subscripts

lim = liquid film when it has attained its limiting thickness

LITERATURE CITED

1. Davies, R. M., and G. I. Taylor, *Proc. Roy. Soc.*, **200A**, 375 (1950).
2. Dumitrescu, D. T., *Z. Angew. Math. Mech.*, **23**, 139 (1943).
3. Griffith, P., and G. B. Wallis, *Trans. Am. Soc. Mech. Engrs.*, **83C**, 307 (1961).
4. Laird, A. E. K., and D. Chisholm, *Ind. Eng. Chem.*, **48**, 1361 (1956).
5. Nicklin, D. J., Ph.D. thesis, Univ. of Cambridge, Cambridge, England (August, 1961).
6. Street, J. R., and M. R. Tek, *A.I.Ch.E.J.*, **11**, No. 4 (1965).
7. White, E. T., and R. H. Beardmore, *Chem. Eng. Sci.*, **17**, 351 (1962).
8. Bretherton, F. P., *J. Fluia Mech.*, **10**, 166 (1961).
9. Walters, J. K., and J. F. Davidson, *ibid.*, **12**, 408 (1962).
10. *Ibid.*, **17**, 321 (1963).
11. Taylor, T. D., and Andreas Acrivos, *ibid.*, **18.**, 466 (1964).
12. Brown, R. A. J., Ph.D. thesis, Univ. of Alberta, Edmonton, Alberta, Canada (May, 1963).
13. Hellums, J. D., and S. W. Churchill, *A.I.Ch.E. Journal*, **10**, 110 (1964).

Manuscript received May 15, 1964; revision received November 18, 1964; paper accepted January 22, 1965. Paper presented at A.I.Ch.E. Houston meeting.

Thermal Conductivity Measurements for Nitrogen in the Dense Gaseous State

DRAGOSLAV MISIC and GEORGE THODOS

Northwestern University, Evanston, Illinois

A coaxial cylindrical type of cell was designed and constructed for the measurement of the thermal conductivity of gases at high pressures and moderate temperatures. This cell was used to establish the thermal conductivity of nitrogen for pressures up to 4,625 lb./sq.in.abs. and for temperatures of 22.2° and 50.5°C. The resulting thermal conductivity values were found to be in agreement with values reported in the literature for nitrogen at these elevated pressures. These experimental measurements indicate that the cell developed for this investigation is capable of producing reliable thermal conductivities for gases at high pressures.

The transport properties of liquids and gases in the dense gaseous state are currently receiving considerable attention from both experimental and theoretical points of view. Predvoditelev (*36*) points out that the transfer of heat through a liquid medium possesses similar characteristics that are comparable to the transfer of heat through dense gases on the one hand and through solids on the other hand. Predvoditelev indicates that a generalized approach to the transport properties is possible. In 1881, Kamerlingh Onnes (*17*) introduced a normalizing parameter to produce a generalized viscosity correlation for gases at atmospheric pressure. Predvoditelev extends and refines this concept and applies it to the thermal conductivity of liquids. Chapman (*5*) and Enskog (*7*) independently developed, from rigorous kinetic theory considerations, expressions for the transport properties of the rare gases. For the effect of pressure on thermal conductivity, Enskog (*8*) presents the relationship

$$\frac{k}{k^*} = b\rho \left[\frac{1}{b\rho\chi} + \frac{6}{5} + 0.7574\, b\rho\chi \right] \qquad (1)$$

where the thermal conductivity of the dilute gas k^* and of the dense gas k are taken at the same temperature. The quantity $b\rho\chi$ is associated with the Enskog equation of state

$$P + \frac{a}{\rho^2} = \frac{RT}{M}\rho\,(1 + b\rho\chi) \qquad (2)$$

More recent work is reported by Kirkwood and Irving (*23*), Kirkwood, Buff, and Green (*22*), Green (*12*), and Snider and Curtiss (*42*). Rice et al. (*37*), using nonequilibrium statistical mechanics, developed the following equation for the thermal conductivity of dense gases:

$$\frac{k}{k^*} = \frac{1}{g(\sigma)}\left\{1 + \frac{7}{5}b\rho g(\sigma) + \frac{12}{25}[b\rho g(\sigma)]^2\right\} \qquad (3)$$

Snider and Curtiss (*42*) derived the following relationship for the effect of pressure on thermal conductivity:

$$\frac{k}{k^*} = \left[1 + \frac{29}{90}n\pi\sigma^3 + \left(\frac{128}{675}\pi + \frac{1}{45}\right)(n\pi\sigma^3)^2\right] \qquad (4)$$

Equation (1) has received the most attention and is found to produce good agreement with experimental values for monatomic and nonpolar diatomic gases.

Basically, three methods have been used for the measurement of thermal conductivities: hot wire method, coaxial cylinders, and parallel plates. In addition, Richter and Sage (*38*) report the use of concentric spheres for the measurement of thermal conductivities of fluids. These methods are characterized with steady operating conditions and possess definite advantages and limitations.

The hot wire method is particularly adapted to measurements at low pressures and has been successfully applied by several investigators (*1, 9, 11, 18, 26, 30, 40, 45, 46, 49, 50, 51*). Stolyarov, Ipatiev, and Teodorovich (*43*) encountered considerable difficulties when applying this method to dense gases in the temperature range of 0° to 300°C. and pressures up to 500 atm. The application of coaxial cylinders for the measurement of thermal conductivity was first introduced by P. W. Bridgman (*3*). This method was later improved by Keyes et al. (*19, 20, 21*) and Guildner (*14*), Comings and co-workers (*24, 27, 28, 29*), Ziebland and Burton (*52*), Johannin (*16*), Rothman and Bromley (*39*), and Uhlir (*48*). The use of the parallel plate method was first reported in 1909 by Todd (*47*) and later by Borovik (*2*) and Nuttall and Ginnings (*35*). This method finds current application only by Michels and co-workers (*31, 32, 33, 34*).

THERMAL CONDUCTIVITY CELL AND EQUIPMENT

The hot wire method has been the least successful of the methods for the measurement of thermal conductivities at high pressures. To obtain reliable values, the dimensions of such a cell are necessarily small and consequently require an extremely high order of precision. The edge effects associated with the parallel plate method present complications that are difficult to minimize. High-pressure data obtained from such a cell by Michels and Botzen (*31*) indicate values that are higher than those obtained by other methods. These differences may be due to convective contributions and edge effects (*16*). Lately, Michels and co-workers (*33, 34*) repeated the measurement of thermal conductivity at high pressures for carbon dioxide, using improvements on the earlier cell, and noted differences over their previous mesurements. Because of the complexity of construction, the concentric spherical type of cell was eliminated from consideration in this study. Instead, the coaxial cylindrical cell was selected for construction because it offers better flexibility of operation and its design allows best the introduction of improvements. The results already obtained by others (*14, 16, 24, 27, 28, 29, 39, 48, 52*) indicate that a coaxial cylindrical cell is most dependable and produces thermal conductivities that are reliable.

Coaxial Cylindrical Cell

The thermal conductivity cell consisted basically of two concentric cylinders with end closures which were provided with high-pressure seals. A cross-sectional view of this high pressure cell is presented in Figure 1. The outside diameter of the outer cylinder was 3⅜ in. and its length was 14 in. Since holes of 1/16-in. diameter having a maximum depth of 5 in. had to be provided with fine thermocouple wires, it became necessary to construct the outer cylinder from two cylindrical shells. In order to assure good thermal contact between these shells so that they would behave as a homogeneous solid, pressure-fitting techniques have been used in the past (*24, 27, 28, 29*). However, for the construction of this cell, advantage was taken only of the thermal expansion characteristics of the material (stainless steel 304) of these two shells. The outer shell was machined and polished to produce a uniform inside diameter of 1.0000 in. On the other hand, the outside diameter of the inner shell, after machining and polishing, was 1.0002 in., thus producing an oversize of 0.0002 in. On the outer surface of the inner shell, two long square grooves, 1/16 in. deep, 1/16 in. wide, and 5 in. long, were spaced and milled diametrically opposite to each other from both ends and were directed to the middle of the shell. In addition, two short square grooves of the same dimensions and ¼ in. deep were also milled in line with the long grooves from the opposite ends as shown in Figure 1. In order to construct the outer cylinder as a single unit from these two shells, the outer shell was heated in a furnace to 400°F., and the inner shell was cooled in liquid nitrogen. The inner shell was then properly telescoped into the outer shell and allowed to reach thermal equilibrium at room temperature, at which conditions these shells were frozen into each other to produce the outer cylinder of the cell. The inside surface of the outer cylinder was then honed and polished to a mirror finish, to an inside diameter of 0.7640 in. within a uniformity of 0.0001 in. over the entire length. Therefore, the thickness of the outer cylinder was ½[3.3750 − 0.7640] = 1.3055 in. and was capable of withstanding easily pressures up to 25,000 lb./sq. in. Four openings spaced 90 deg. apart were provided on each end of the outer cylinder for accommodating the electrical leads to the cell. Two of the electrode openings are shown on the left side of the cell in Figure 1. The sample gas inlet was located between two electrical lead outlets and was axially offset from the electrode openings. This arrangement forced the gas to be detoured and to be introduced into the annular space from the end of the cell.

The inner cylinder was also constructed from two shells (stainless steel 304) with the same technique used as outlined for the construction of the outer cylinder. The shells of the inner cylinder had the following dimensions:

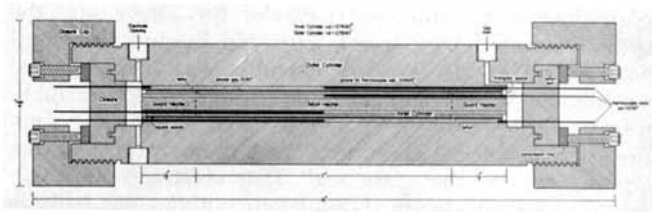

Fig. 1. Cross-sectional view of high-pressure thermal conductivity cell.

inner shell, I.D. = 0.3125 in., O.D. = 0.5397 in.; outer shell, I.D. = 0.5395 in. and O.D. = 0.7440 in. after polishing to a mirror finish. The cylindrical space of the inner cylinder housed the heating elements of the cell. The inner shell was provided on each end with three thermocouple grooves, 1/16 in. deep and 1/16 in. wide. One of these three thermocouple grooves (shown in Figure 1) was made 5 in. deep to match the corresponding deep thermocouple groove of the outer cylinder. The other two thermocouple grooves were positioned 45 and 90 deg. from their long groove, and the grooves corresponding to the same length on the opposite end of the inner cylinder were offset by 180 deg. The central portion of the inner cylinder (approximately 7 in.) was used as the test section and was provided on both ends with guard sections (each approximately 1½ in. long). In order to establish boundaries and to reduce axial heat conduction for the test section, circular square grooves, 1/16 in. wide, were machined out from the surface of the inner cylinder to a depth corresponding to the thickness of the outer shell. These circular grooves were filled with Teflon rings in order to minimize the possibility of natural convection in this space. The two shorter thermocouple grooves of the inner cylinder extended to a distance in front and after the Teflon filled grooves.

The inner and outer cylinders separated with an annular gap of 0.0100 in. were aligned concentrically by means of two ring spacers also made of stainless steel 304 and located at the end of each guard section. To minimize contact between the two cylinders, one ring spacer was of a rectangular design, while the other was triangular in shape, with each contact having an area of approximately 1/16 × 1/16 in. The alignment of these cylinders was checked by optical means.

Closures at the ends of the cell were held in place with closure caps provided with six 5/16-in. bolts which acted on a compression ring. The compression ring was annealed and was used to transmit a uniform force on the end closures. A circular groove on the closure was filled with a Teflon ring and was pressed tight with the bolts against the corresponding square circular ridge of the outer cylinder in order to properly seal the cell. Thermocouple wells, (O.D. = 0.051 in. and I.D. = 0.033 ± 0.002 in.) made from 316 stainless steel seamless tubing were inserted through properly located holes in the end closure to match the corresponding thermocouple grooves located in the inner and outer concentric cylinders. These wells were silver soldered to the end closure with induction heating to produce seals capable of withstanding high pressures. These thermocouple wells were accommodated with stainless steel shielded copper-constantan thermocouples (O.D. = 0.025 ± 0.002 in.). This arrangement permitted easy access and replacement of thermocouples.

In order to introduce the electric energy to the main and guard heaters, electrodes had to be designed to prevent current and pressure leakages. Each electrode was constructed by first surrounding a wire with glass tubing, which in turn was covered with a metallic sleeve. One end of the sleeve was fused to the electrode with a glass bead to produce a pressure seal between the sleeve and the centrally located wire which extended beyond the fused glass seal. This glass sealed assembly was then inserted in a standard stainless steel tubing provided with a high-pressure fitting. The sleeve and stainless steel tubing were then silver soldered to form a high-pressure seal at the opposite end of the glass seal. This electrode assembly offered excellent electrical insulation without gas leakage for pressures as high as 15,000 lb./sq. in. and temperatures limited only by the melting point of the glass.

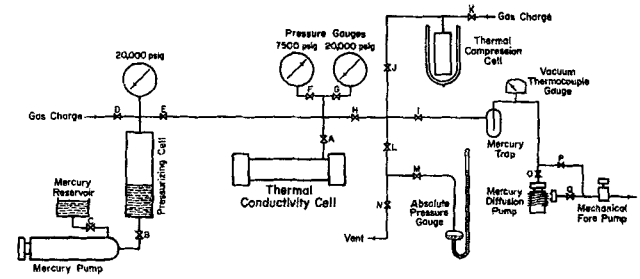

Fig. 2. Schematic diagram of experimental unit for thermal conductivity studies.

The main and guard heaters were constructed out of a ceramic material which was machinable. These ceramic rods were machined to a diameter of 0.3120 in. and were threaded on their surface with eighteen grooves per inch to a depth of 0.027 in. The main heater rod was solid throughout and was 7 in. long, while each guard heater was provided in the center with a 3/16-in. hole to accommodate the electrical leads of both the main and guard heaters. Each guard heater rod was 1½ in. long. Nichrome wire, O.D. = 0.010 in. and having an electrical resistance of 6.56 ohms/ft., was wound in the grooves of the main and guard heater rods and was covered with saureisen cement to freeze it in place and provide electrical insulation. From each end of the main heater, two copper leads, insulated individually with ceramic tubing, were provided and were passed through the hollow center of each guard heater. One set of these leads was connected to a potentiometer to measure the voltage drop across the main heater, while the other set was used to provide the electric current into the main heater. Each guard heater was provided with the same type of nichrome wire with one end of the wire being returned through the center hole of this heater. Therefore, four wires were present on the end of each guard heater. These leads were then passed through a Teflon wafer provided with properly spaced holes to accommodate the gas inlet, thermocouple wells, and the electric wires leaving each guard heater. These wires were then soldered to the electrodes and were bent so no contact would be made with the thermocouple wells. An additional wafer made of the same ceramic material and provided with the necessary openings was placed to cover the soldered connections and to fill up as much of the free space. The Teflon and ceramic wafers are not shown in Figure 1. This basically constituted the procedure necessary for preparing the cell before installing the end closures to the thermal conductivity cell.

A schematic diagram of the experimental unit is presented in Figure 2. The basic components of this unit can be resolved into the pressurizing system, the evacuating system, the electrical energy supply system, and other auxiliary instruments necessary for making thermal conductivity measurements.

Pressurizing System

The high-pressure equipment used in connection with the thermal conductivity cell includes the following: mercury reservoir, pressurizing pump, pressurizing cell, thermal compression cell, pressure gauges, and necessary valves, fittings, and tubing. The pressurizing pump is a positive displacement pump having a capacity of 100 cc. and a maximum working pressure of 25,000 lb./sq. in. Mercury was introduced into the pump from the reservoir through valve *C* which was closed thereafter. The gas was charged into the pressurizing cell through valve *D*, with valve *E* closed, after the whole system had been

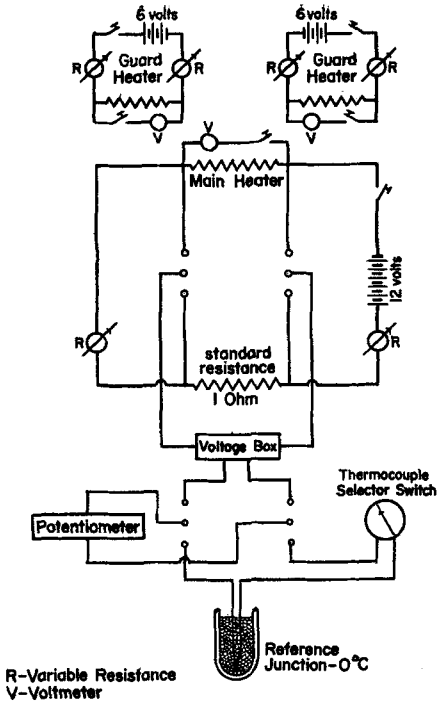

Fig. 3. Schematic diagram of electrical circuits.

evacuated. The mercury of the pressurizing cell forms a liquid piston that can compress the gas throughout the entire system. The pressurizing cell was made of stainless steel 316 and had a capacity of approximately 105 cc. and a maximum working pressure of 15,000 lb./sq. in. at 100°F. To avoid the possibility of mercury overflow from the pressurizing cell, an electrode was located on the top part of the pressurizing cell, so when the mercury level reached the electrode, a warning circuit was closed and an alarm rang. The thermal compression cell was identical to the pressurizing cell. After evacuating the cell, valve *J* was closed and the gaseous sample was charged through valve *K*. For gases not available at high pressures, this cell was surrounded with a liquid nitrogen bath to transfer and condense a prescribed quantity of the gas into it. Upon allowing this cell to reach room temperature, the gas became available at high pressures, and thus it could be charged directly into the thermal conductivity cell or the pressurizing cell where it could be further compressed. The two pressure gauges (7,500 and 20,000 lb./sq. in. gauge) were periodically checked with a dead weight gauge. Pressures could be read accurately to within 5 and 10 lb./sq. in., respectively. In order to measure pressures near 1 atm. or less, an absolute pressure manometer was attached to the equipment.

Evacuating System

A mechanical fore pump connected in series with a mercury diffusion pump provided the basic evacuating facilities for the system. A vacuum thermocouple gauge provided means for detecting pressures as low as 5 μ.

Electrical System

A schematic diagram of the electrical circuits used for supply and measurements is shown in Figure 3. The main heater (approximately 36 ohms) was connected in series to a 12 v. heavy duty battery, a 1 ohm standard resistance, and two variable resistances. With a double pole–double throw switch, the voltage drop across the 1-ohm standard resistance and across the main heater was measured with a K-3 potentiometer. The voltage drop across the standard 1-ohm resistance represents directly the current through the main heater. Each guard heater (approximately 8.5 ohms each) was also connected in series with a 6-v. battery and two variable resistances for coarse and fine adjustments. Voltmeters in these circuits were used only as indicating instruments. A voltage box was used to reduce the available 12 v. of the main circuit to the measuring capabilities of the potentiometer. A similar double pole–double throw switch connected the electrical supply and temperature measuring thermocouple wires to the K-3 potentiometer. With this arrangement, the voltage drop and current through the main heater were kept constant to 0.0001 v. for a run requiring several hours.

The copper-constantan thermocouples were used as the temperature sensing devices and were calibrated against a certified platinum resistance thermometer with a bridge assembly. The calibration of the thermocouples was frequently checked and found to remain unchanged over the entire period of these studies. Ice water was used as the reference junction to these thermocouples.

EXPERIMENTAL PROCEDURE

The assembled cell was immersed in a constant temperature bath having a volume capacity of 50 gal. The operating temperature range was −29° to +83°C. and was capable of maintaining control to within ±0.01°C.

The charging procedure varied with the gas and the available cylinder pressure. To begin this operation, a predetermined amount of nitrogen at high pressures was introduced into the pressurizing cell, where it was expanded down to approximately 70 to 80 lb./sq. in. abs. The expanded gas was then slowly introduced through valves *E* and *A* into the thermal conductivity cell. The pressure of the gas was then increased through the introduction of mercury into the pressurizing cell. This procedure was carried out as often as was necessary in order to establish the desired pressure in the cell. The pressurized cell was allowed to reach thermal equilibrium with the bath until the thermocouples registered no change in temperature with time. At this stage, the main and both guard heaters were turned on, and adjustments were made until no axial temperature gradient existed. Ordinarily, temperature equilibrium was obtained at approximately 30 min. after final main heater and guard heater adjustments were made. Temperature measurements were then made on all thermocouples at 10-min. intervals for approximately 1 hr. Simultaneously, readings were obtained on the voltage and current through the main heater, and the pressure of the system. After a set of readings was obtained, the pressure of the system was increased, and a new set of readings corresponding to this pressure was established. This procedure was continued until the maximum desired pressure was reached. The same measurements were repeated with decreasing pressure, and no hysteresis effects were encountered. During these operations, the bath temperature was kept constant. If the gas to be used was condensable with liquid nitrogen, and was not available at sufficiently high pressures, the thermal compression cell was employed for charging. For methane, usually available at 1,100 lb./sq. in., this approach can be used to obtain pressures as high as 10,000 lb./sq. in.

ANALYSIS OF DATA

The interpretation of the experimental measurements follows the pattern outlined for radial heat conduction through a series of cylindrical walls of infinite length. For the coaxial thermal conductivity cell, the total heat flow by conduction becomes

$$Q = \frac{\Delta T}{\frac{\ln(r_1/r_0)}{2\pi k_m L} + \frac{\ln(r_2/r_1)}{2\pi k L} + \frac{\ln(r_3/r_2)}{2\pi k_m L}} \qquad (5)$$

The gas gap is defined in the radial interval r_1 to r_2. The

thermal conductivity of stainless steel 304 as a function of temperature is taken from Brown (*4*) as

$$k_m = 8.1 + 0.0045t \quad (6)$$

Values obtained with Equation (6) were converted to cal./sec. cm. °K. After making the necessary substitutions for r_0, r_1, r_2, and r_3 in Equation (5) and solving for k, one gets

$$k = 422.16 \times 10^{-5} \frac{Q}{L\Delta T - 0.10374 \frac{Q}{k_m}} \quad (7)$$

The total heat flow Q, calories per second, was obtained from the measurement of voltage and current as

$$Q = JEI \quad (8)$$

In these studies, the voltage was varied from 6 to 12 v., while the current varied from 0.15 to 0.30 amp. The maximum temperature difference ΔT never exceeded 1.2°F. These conditions practically eliminated any radiation and convective contributions. The effect of radiation was calculated to be less than 0.1%, while the contribution due to convection never exceeded 0.5% of the total heat transfer. The criterion for natural convection in gases was introduced by Kraussold (*25*) as the ratio of the apparent to the true thermal conductivity as follows:

$$\frac{k_a}{k} = f\left[\frac{l^3 g \rho^2 \beta \Delta T}{\mu^2} \cdot \frac{c_p \mu}{k}\right] = f[N_{Gr} \times N_{Pr}] \quad (9)$$

When the product $N_{Gr} \times N_{Pr} < 1{,}000$, then $k_a/k = 1.00$. These conditions were always satisfied, and consequently the effect of natural convection was not assumed to be present, since the product $N_{Gr} \times N_{Pr}$ in these studies was always less than 100. These contributions are within the experimental limits of this study, which are estimated to be ± 1.5%.

The measured length of the test section (L = 6.875 in.) was used with Equation (7) to calculate the thermal conductivity of nitrogen at atmospheric pressure and temperatures of 22.2° and 50.5°C. These calculated thermal conductivities were found to be slightly higher than the average values resulting from the work of a number of investigators presented in the literature (*6, 10, 11, 13, 15, 16, 21, 28, 29, 31, 35, 39, 41, 43, 44, 49, 50*). As a result, the average thermal conductivity value of nitrogen was taken as most reliable and was used to obtain the effective length of the test section. This length was then used with Equation (7) to calculate the thermal conductivity values of nitrogen at any pressure. In order to account for the effect of pressure on the cell dimensions, a correction was applied to these calculated thermal conductivity values. This pressure correction included the properties of the stainless steel such as Young's modulus and Poisson's ratio, and the pertinent cell dimensions. This correction was found to be

$$k = k_a [1 + 2.464 \times 10^{-6} P] \quad (10)$$

The resulting thermal conductivity values for nitrogen are presented in Table 1 at 22.2° and 50.5°C. and for pressures up to 4,625 lb./sq. in. abs. These experimental values were fitted by means of the method of least squares to produce the following relationships:

$$k \times 10^6 = 6.203 + 0.9256 \times 10^{-3} P + 0.0203 \times 10^{-6} P^2 \quad \text{at 22.2°C.} \quad (11)$$

and

$$k \times 10^5 = 6.641 + 0.5225 \times 10^{-3} P + 0.1460 \times 10^{-6} P^2 - 0.0154 \times 10^{-9} P^3 \quad \text{at 50.5°C.} \quad (12)$$

Equations (11) and (12) have been used to calculate thermal conductivity values at the corresponding experimental pressures and are also presented in Table 1. A comparison of the experimental thermal conductivities and the relationships of Equations (11) and (12) are presented in Figure 4 for nitrogen at 22.2° and 50.5°C.

TABLE 1. THERMAL CONDUCTIVITY VALUES OF NITROGEN

P, lb./sq. in. abs.	k, cal./sec. cm. °K. Exptl.	Calc.	$k-k^*$	ρ_R
	22.2°C. ($k^* = 6.19 \times 10^{-5}$)			
899	7.08×10^{-5}	7.05×10^{-5}	0.89×10^{-5}	0.225
1,510	7.63	7.64	1.44	0.371
2,183	8.25	8.32	2.06	0.536
3,005	9.17	9.17	2.98	0.720
3,515	9.78	9.71	3.59	0.820
3,737	9.96	9.95	3.77	0.863
4,100	10.33	10.34	4.14	0.921
4,625	10.89	10.92	4.70	1.01
	50.5°C. ($k^* = 6.64 \times 10^{-5}$)			
1,000	7.41	7.29	0.77	0.230
1,298	7.41	7.53	0.77	0.295
1,600	7.75	7.79	1.11	0.357
1,907	7.98	8.06	1.34	0.422
2,215	8.38	8.35	1.74	0.483
2,530	8.68	8.65	2.04	0.550
2,830	9.12	8.94	2.48	0.610
3,105	9.14	9.21	2.50	0.663
3,400	9.55	9.50	2.91	0.712
3,735	9.81	9.83	3.17	0.767
4,012	9.97	10.09	3.33	0.820
4,275	10.29	10.34	3.65	0.862
4,617	10.74	10.65	4.10	0.920

In order to compare the high pressure thermal conductivity measurements of this study with values reported in the literature for nitrogen, the residual thermal conductivity $k - k^*$ was plotted against ρ_R, the reduced density. The results of this comparison are presented in Figure 5. Altogether nine references (*16, 19, 21, 24, 28, 29, 35, 43, 49*) were consulted, and their results are presented in this figure along with the data obtained from this investigation. It will be noted that this type of correlation does not show directly the effect of temperature and pressure, since these variables have been used to define the reduced density of the substance. In order to obtain values

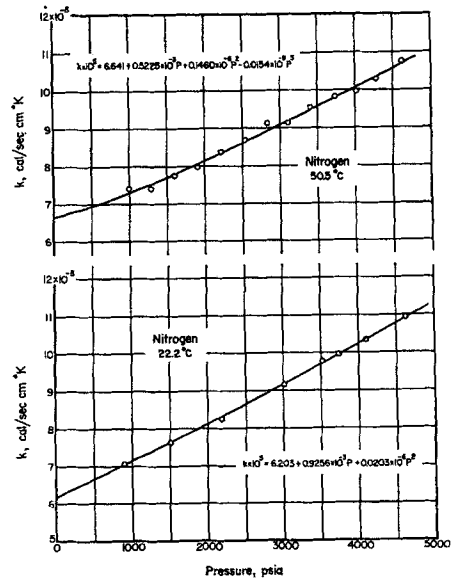

Fig. 4. Pressure dependence of thermal conductivity for nitrogen at 22.2° and 50.5°C.

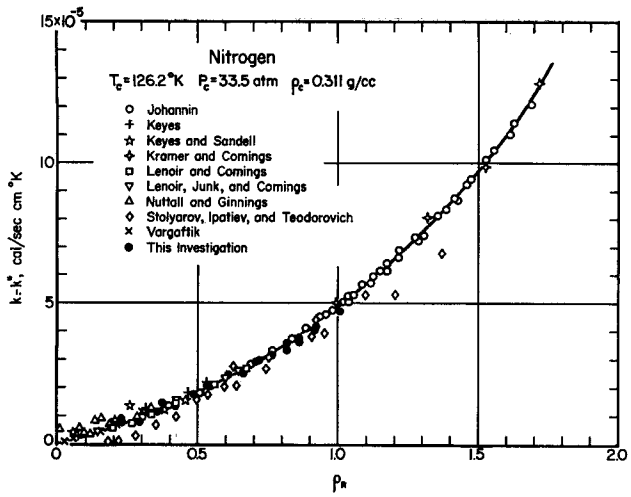

Fig. 5. Residual thermal conductivity vs. reduced density relationship for nitrogen.

of $k - k^*$ that are consistent with each reference, the low pressure (1 atm.) k^* values presented in the respective references were used. It is of interest to note that a $k - k^*$ vs. ρ_R plot is unique and can be expressed as a single monotonic function despite the fact that the temperature and pressure can vary over wide ranges. This fact is well substantiated with the very precise data of Johannin (*16*) for nitrogen, which cover a temperature variation of 75° to 700°C. and pressures from 1 up to 1,600 atm. In this comparison, the data of Comings et al. (*24, 27, 28, 29*) appear to be in good agreement. The thermal conductivity measurements of Michels and Botzen (*31*) have not been included in Figure 5. Their data were found to be consistently higher, particularly in the dense gaseous region. This fact is also pointed out by Johannin (*16*). The experimental results of this investigation are in good agreement with the relationship of Figure 5 and are consistent with the better work of Johannin (*16*) and Comings et al. (*24, 27, 28, 29*). A review of Figure 5 indicates that considerable scattering is encountered with several references, particularly in the less dense region. This fact should not downgrade the efforts of a number of respectable references, but instead it should serve to point out the extreme experimental difficulties encountered in the procurement of these basic data that are so necessary to establish the proper behavior of this transport property.

CONCLUSIONS

The coaxial cylindrical thermal conductivity cell designed and constructed for this investigation is capable of producing reliable thermal conductivities for gases at moderate temperatures and high pressures. This coaxial cell was tested for reliability with nitrogen at 22.2° and 50.5°C. and pressures up to 4,625 lb./sq. in. abs. The thermal conductivity measurements at these two temperatures were found to be in good agreement with experimental values reported in the literature. This fact should add credence to the dependability of a coaxial cylindrical cell for the measurement of reliable thermal conductivity values of gases at elevated pressures.

ACKNOWLEDGMENT

The authors gratefully acknowledge the financial support of the Petroleum Research Fund of the American Chemical Society through Grant 329-A which has made this study possible.

NOTATION

a,b = constants, Equations (1), (2), and (3)
c_p = heat capacity, cal./g. °K.
E = electrical potential, v.
g = gravitational acceleration, 980.7 cm./sec.^{2}
$g(\sigma)$ = local equilibrium pair correlation function
N_{Gr} = Grashof number, $l^3 g \rho^2 \beta \Delta t / \mu^2$
I = current, amp.
J = conversion factor, 0.23897 cal./sec. w.
k^* = thermal conductivity of gas at atmospheric pressure, cal./sec. cm. °K.
k = thermal conductivity, cal./sec. cm. °K.
k_a = apparent thermal conductivity, cal./sec. cm. °K.
k_m = thermal conductivity of metal, cal./sec. cm. °K.
l = gas gap, cm.
L = length of cell test section, cm.
M = molecular weight
n = constant, Equation (4)
P = pressure
N_{Pr} = Prandtl number, $c_p \mu / k$
Q = heat flow, cal./sec.
r = radius, cm.
R = gas constant, 82.055 cc. atm./g.-mole °K.
t = temperature, °F.
T = absolute temperature, °K.

Greek Letters

β = coefficient of thermal expansion, reciprocal temperature
μ = viscosity, g./cm. sec.
ρ = density, g./cc.
ρ_c = critical density, g./cc.
ρ_R = reduced density, ρ/ρ_c
π = constant, 3.1416
χ = collision diameter, cm.
σ = probability of nearness, Equations (1) and (2)

LITERATURE CITED

1. Abas-zade, A. K. Doklady, *Akad. Nauk Azerbaidzhan SSR*, 3, 3 (1947).
2. Borovik, E., *Zhur. Eksptl. i Teoret. Fiz.*, **17**, 328 (1947).
3. Bridgman, P. W., *Proc. Am. Acad. Arts Sci.*, **59**, 141 (1923).
4. Brown, G. G., and Associates, "Unit Operations," p. 584, Wiley, New York (1950).
5. Chapman, Sydney, *Phil. Trans. Roy. Soc.*, **A216**, 279 (1916).
6. Dickins, B. G., *Proc. Roy. Soc.* (*London*), **A143**, 517 (1934).
7. Enskog, David, Dissertation, Upsala, Sweden (1917).
8. ———, *Svensk. Akad. Handl.*, 63, No. 4 (1922).
9. Eucken, A., *Physik. Z.*, **12**, 1101 (1911).
10. *Ibid.*, **14**, 324 (1913).
11. Frank, E. U., *Z. Elektrochem.*, **55**, 636 (1951).
12. Green, H. S., "Molecular Theory of Fluids," Interscience, New York (1952).
13. Gregory, Hamar, and Sybil Marshall, *Proc. Roy. Soc.* (*London*), **A114**, 354 (1927).
14. Guildner, L. A., "Transport Properties in Gases," p. 55, Northwestern Univ. Press, Evanston, Illinois (1958).
15. Hilsenrath, Joseph, C. W. Beckett, W. S. Benedict, Lilla Fano, H. J. Hoge, J. F. Masi, R. L. Nuttall, Y. S. Touloukian, and H. W. Woolley, "Tables of Thermal Properties of Gases," National Bureau of Standards Circ. 564 (1955).
16. Johannin, Pierre, Doctoral thesis, Univ. of Paris, France (1958).
17. Kamerlingh Onnes, H., *Verhand. Akad. Amsterdam*, **21**, 2de Stuk, 8 (1881).
18. Kannuluik, W. G., and L. H. Martin, *Proc. Roy. Soc.* (*London*), **A144**, 496 (1934).
19. Keyes, F. G., *Trans. Am. Soc. Mech. Engrs.*, **73**, 603 (1951).
20. *Ibid.*, **74**, 1303 (1952).

21. ———, and D. J. Sandell, *ibid.*, **72**, 767 (1950).
22. Kirkwood, J. G., F. P. Buff, and H. S. Green, *J. Chem. Phys.*, **17**, 988 (1949).
23. Kirkwood, J. G., and J. H. Irving, *ibid.*, **18**, 817 (1950).
24. Kramer, F. R., and E. W. Comings, *J. Chem. Eng. Data*, **5**, 462 (1960).
25. Kraussold, H., *Forsch. Gebiete Ingenieurw.*, **5**, 186 (1934).
26. Lambert, J. D., K. J. Cotton, M. W. Pailthorpe, A. M. Robinson, J. Scrivens, W. R. F. Vale, and R. M. Young, *Proc. Roy. Soc. (London)*, **A231**, 280 (1955).
27. Leng, D. E., and E. W. Comings. *Ind. Eng. Chem.*, **49**, 2042 (1957).
28. Lenoir, J. M., and E. W. Comings, *Chem. Eng. Progr.* **47**, 223 (1951).
29. Lenoir, J. M., W. A. Junk, and E. W. Comings, *ibid.*, **49**, 539 (1953).
30. Mann, W. B., and B. G. Dickens, *Proc. Roy. Soc. (London)*, **A134**, 77 (1931).
31. Michels, A., and A. Botzen, *Physica*, **18**, 605 (1952).
32. ———, A. S. Friedman, and J. V. Sengers, *ibid.*, **22**, 121 (1956).
33. Michels, A., J. V. Sengers, and P. S. Van der Gulik, *ibid.*, **28**, 1201 (1962).
34. *Ibid.*, 1216.
35. Nuttall, R. L., and D. G. Ginnings, *J. Res. Natl. Bur. Standards* 58, 271 (1957).
36. Predvoditelev, A. S., *J. Phys. Chem.* (U.S.S.R.), **22**, 339 (1948).
37. Rice, S. A., J. G. Kirkwood, John Ross, and R. W. Zwanzig, *J. Chem. Phys.*, **31**, 575 (1959).
38. Richter, G. N., and B. H. Sage, *Chem. Eng. Data Series*, **2**, 61 (1957).
39. Rothman, A. J., and L. A. Bromley, *Ind. Eng. Chem.*, **47**, 899 (1955).
40. Schleirmacher, A., *Ann. Physik.*, **26**, 287 (1885).
41. Schottky, W. F., *Z. Elektrochem.*, **56**, 889 (1952).
42. Snider, R. F., and C. F. Curtiss, *Phys. Fluids*, **1**, 122 (1958).
43. Stolyarov, E. A., V. V. Ipatiev, and P. Teodorovich, *Zhur. Fiz. Khim.*, **24**, 166 (1950).
44. Stops, D. W., *Nature*, **164**, 966 (1949).
45. Taylor, W. J., and H. L. Johnston, *J. Chem. Phys.*, **14**, 219 (1946).
46. Thomas, L. B., and R. C. Golike, *ibid.*, **22**, 300 (1954).
47. Todd, G. W., *Proc. Roy. Soc. (London)*, **A83**, 19 (1909).
48. Uhlir, A., *J. Chem. Phys.*, **20**, 463 (1952).
49. Vargaftik, N. B., *Zhur. Tekh. Fiz.*, **4**, 341 (1937).
50. ———, and E. V. Smirnova, *ibid.*, **26**, 1251 (1956).
51. Vines, R. G., *Australian J. Chem.*, **6**, 1 (1953).
52. Ziebland, Hans, and J. T. A. Burton, *Inst. J. Heat Mass Transfer*, **1**, 242 (1960).

Manuscript received October 14, 1964; revision received January 5, 1965; paper accepted January 7, 1965. Paper presented at A.I.Ch.E. San Francisco meeting.

The Effect of Concentration Level on the Gas Phase Absorption Coefficient

J. EDWARD VIVIAN and WILLIAM C. BEHRMANN

Massachusetts Institute of Technology, Cambridge, Massachusetts

A theoretical and experimental investigation has been made to determine the effect of the concentration level on the rate of mass transfer of a solute from a nontransfering or inert carrier gas in turbulent flow.

Diffusion theory predicts the gas phase mass transfer coefficient to be inversely proportional to the first power of the mean mole fraction of the nontransferring gas and to be a possible function of the rate and direction of mass transfer.

The results of an experimental study of the absorption of ammonia from mixtures with nitrogen into distilled water and aqueous ammonia solutions in a short wetted-wall column verified the predicted inverse relationship between the turbulent gas phase absorption coefficient and the first power of the mean inert mole fraction for inert mole fractions ranging from 0.068 to 0.934. The data also showed that for the range covered in this investigation there was no significant influence of the mass transfer rate on the product of the coefficient and the mean mole fraction of the inert carrier gas.

In chemical engineering operations such as gas absorption, evaporation into gas streams, and partial condensation the mass transfer in the gas phase may often be characterized as a process involving the diffusion of a solute through a nontransferring carrier gas between a dense boundary and a turbulent core. Heretofore, the effect of the concentration level on the transfer rate in this type of system has been taken into account in design by the use of the predictions of film theory based on the well-established effect of concentration level on mass transfer by molecular diffusion (*16*). Recent attempts to verify the predictions of film theory for evaporation into turbulent gas streams, however, have yielded conflicting results with respect to the correct relationship between the concentration level and the mass transfer coefficient. To obtain a better understanding of the phenomenon, this study applies the basic knowledge currently available on turbulent transfer processes and tests

William C. Behrmann is with Esso Research and Engineering, Baton Rouge, Louisiana.